An Ultra-Low Power Dual-mode ECG Monitor for Healthcare and Wellness

Daniele Bortolotti[†], Mauro Mangia[‡], Andrea Bartolini[†§], Riccardo Rovatti[†‡], Gianluca Setti[*‡] and Luca Benini[†§]
[†]DEI, [‡]ARCES, University of Bologna, Italy - Email: {daniele.bortolotti, mauro.mangia2, riccardo.rovatti}@unibo.it
[§]Integrated Systems Laboratory, ETH Zurich, Switzerland - Email: {barandre, lbenini}@iis.ee.ethz.ch
[*]ENDIF, University of Ferrara, Italy - Email: gianluca.setti@unife.it

***Abstract*—Technology scaling enables today the design of ultra-low cost wireless body sensor networks for wearable biomedical monitors. These devices, according to the application domain, show greatly varying tradeoffs in terms of energy consumption, resources utilization and reconstructed biosignal quality. To achieve minimal energy operation and extend battery life, several aspects must be considered, ranging from signal processing to the technological layers of the architecture. The recently proposed Rakeness-based Compressed Sensing (CS) expands the standard CS paradigm deploying the localization of input signal energy to further increase data compression without sensible RSNR degradation. This improvement can be used either to optimize the usage of a non volatile memory (NVM) to store in the device a record of the biosignal or to minimize the energy consumption for the transmission of the entire signal as well as some of its features. We specialize the sensing stage to achieve signal qualities suitable for both Healthcare (HC) and Wellness (WN), according to an external input (e.g. the patient). In this paper we envision a dual-operation wearable ECG monitor, considering a multi-core DSP for input biosignal compression and different technologies for either transmission or local storage. The experimental results show the effectiveness of the Rakeness approach (up to $\approx 70\%$ more energy efficient than the baseline) and evaluate the energy gains considering different use case scenarios.**

I. Introduction and Related Work

Heart activity monitoring is of primary interest in a large set of human habits. Today cardiovascular diseases or lifestyle-induced diseases, so-called non-communicable diseases, are becoming severe and affecting a growing portion of the world population. In general, human behavior-related illness requires accurate and long-term medical supervision, which is unsustainable for the traditional healthcare system due to increasing costs and medical management resources needed [1]. Personal health monitoring systems are able to offer a large-scale and cost-effective solution to this problem. Wearable, miniaturized and Wireless Sensors Network (WSN) nodes to continuously measure and remotely report biomedical signals, can indeed provide the ubiquitous, long-term and real-time monitoring required by the patients and enable faster coordination with medical personnel. Such healthcare applications need the emergence of new technologies to allow the development of extremely power-efficient bio-sensing nodes and rely on the capability of the electronic market and the research community to provide ultra-low/zero power systems with adequate performance.

Holter monitors and loop recorder devices are today used for medical grade ECG recording [7], while reduced leads ECG monitors are used for lifestyle heart rate monitoring, which includes sport activity trackers, obesity and stress detectors. Historically these devices have been addressed separately since their intrinsic different ECG reconstruction quality and battery lifetime requirements had led to different architectures. A Holter monitor is a device that continuously records the cardiac rhythm. Electrodes (small conductive patches) are placed onto the patient chest and attached by wires to the recording monitor. The monitor runs on batteries and it is worn for 24 - 48 hours during normal activity. ECG loop recorders are implantable devices capable of storing data automatically in response to a significant arrhythmia or in response to patient activation. It is particularly useful either when symptoms are infrequent or when aggregate long-term data are required. In the WSN context, new and forthcoming solutions for wearable devices offer medical grade ECG monitoring and high-quality transmission to personal servers such as smartphones [4], thus enabling new horizons for health through mobile technologies [6]. On the other hand lifestyle ECG monitors, which are rapidly evolving into mass products [5], have completely different requirements, mostly centered on an extended battery life.

Compressed Sensing (CS) signal acquisition and compression paradigm [9], has proved to be an energy efficient approach suitable for embedded biomedical monitors [3], [2], [8]. The aim of CS is to represent the information content of the input signal using fewer digital words with respect to Nyquist-rate sampling. The general CS theory was recently extended with the introduction of the concept of *rakeness* [14]. The basic idea behind this approach is to exploit localization of signals, i.e. the assumption that the information of the signal is not equally distributed in its domain. Roughly speaking, localization implies that some realizations of the input process have a higher probability with respect to others.[1] In [14] authors showed that the specialization of the CS approach over classes of localized signals allows to achieve either a higher quality of the reconstructed signal or a increased data compression necessary to target a given reconstruction quality.

In a typical wearable biomedical monitoring system based on CS, three phases can be identified: (i) input biosignals acquisition, (ii) sensors data processing and finally (iii) management of the processed input. In the first stage the analog input biosignal is sampled and made available to a digital signal processor (DSP) for processing. Subsequently the com-

[1]the hypothesis of localization is not a limitation since the only class of signals where all possible realizations have the same probability is white noise.

978-3-9815370-4-8/DATE15/©2015 EDAA

pressed output can be transmitted (to a personal server such as a smartwatch or smartphone) or locally stored for later off-line medical analysis. Motivated by the inherent parallel nature of medical grade biomedical monitoring, where multi-channel signal analysis is suitable for parallel processing, a multi-core DSP is considered in this work [18]. From a technological point of view, emerging Non Volatile Memories (NVM) allow to have on-chip low-power storage, suitable for keeping a record of medical grade compressed ECG data in the device. As a matter of fact, it is of utmost importance from a medical point of view to record the triggering event from a normal heart activity to a suspicious activity that requires medical investigations and supervision.

In this work we present a unified architecture capable of offering signal qualities suitable for both medical grade and lifestyle applications leveraging the quality offered by the rakeness-based CS. The envisioned dual-mode ECG monitor is able to handle in highly energy efficient way different application scenarios, such as healthcare and wellness, according to an external trigger. The main contributions of this paper are the following:

- we present an ultra-low power dual-mode ECG monitor, suitable for *Healthcare* applications, where medical grade signal quality is needed, and for *Wellness* applications where heart rate detection suffices. An external input (e.g. patient) enables the transition between the two operating modes.
- the different levels of quality needed for healthcare and wellness scenarios are enabled by the wider reconstruction quality / compression enabled by the rakeness-based CS. The rakeness-based CS leads to $\approx 55\%$ improvements w.r.t. standard CS and can substantially increase ($\approx 82\%$) the data compression in a healthcare scenario, while for wellness applications the energy efficiency is up to $\approx 77\%$ with more than 120% in data compression improvements;
- to complete the analysis, we analyzed the energy gains including transmission and storage impact, considering different possible use cases scenarios and varying the amount of time spent in healthcare/wellness configuration.

The rest of the paper is organized as follows. In Section II the rakeness-based compressed sensing approach is introduced. Section III presents the dual-mode ECG monitoring system. Next, in Section IV we describe the experimental setup and the results of the evaluation in terms of reconstruction quality, energy efficiency considering different application scenarios. Finally, the conclusions are presented in Section V.

II. Rakeness-based Compressed Sensing

Compressed Sensing (CS) is a recently introduced paradigm allowing the reconstruction of a signal instance starting from a set of properly designed linear non-adaptive measurements that are potentially much smaller than the number of samples at the signal Nyquist rate. The possibility of going sub-Nyquist hinges on a prior knowledge on the considered class of input signals, which must be sparse: many real-world signals are such that, if expressed along a suitable basis exhibit a large number of zero or almost zero components. For a generic time window T, we use the vector x to represent the N Nyquist-rate input signal samples, sparse means that, with $x = \Psi\alpha$ where Ψ is a $N \times N$ matrix representing the sparsity basis, the coefficients vector α has at most K non null elements with $K \ll N$. The aim of CS is to represent each signal instance with a proper measurement vector y, composed by M different digital words that are less than N [11].

The input signal information extraction is achieved by a set of N-dimensional sensing vectors ϕ_j, $j = 1, \ldots, M$ arranged row by row in the sensing matrix Φ such that:

$$y = \Phi x + \nu = \Phi\Psi\alpha + \nu = A\alpha + \nu \tag{1}$$

where $A = \Phi\Psi$ is a $M \times N$ matrix that link the sparse representation α with y. ν is an additive noise that takes into account all the non-idealities of the system (quantization error or intrinsic input signal noise).

The problem of reconstruction α (and thus $x = \Psi\alpha$) translates in the inversion of the rectangular operator A. This is an ill-posed problem, consequently, there are infinite realization α such that $A\alpha = y$. To overcome this impasse the CS theory [9] adopts as the candidate for signal reconstruction the sparsest vector $\hat{\alpha}$ mapped into y by A. Algorithmically, the simplest option is to solve the following optimization problem:

$$\begin{aligned} \hat{\alpha} &= \min \|\alpha\|_{l1} \\ \text{s.t. } & \|\Phi\Psi\alpha - y\|_{l2} < \epsilon \end{aligned} \tag{2}$$

where $\|\cdot\|_{l_1} = \sum|\cdot|$ and $\|\cdot\|_{l_2} = \sum\cdot^2$ are the standard l_1 and l_2 norms, ϵ bounds the effects of the noise ν and the reconstructed signal can therefore be written as $\hat{x} = \Psi\hat{\alpha}$ [9]. The goodness of the reconstruction is guaranteed by the Restricted Isometry Property (RIP) [12] of the matrix A, ensuring that the sensing stage is able to conserve the input signal l_2 norm also with $M < N$. The CS theory guarantees that for all possible sensing matrices RIP is always satisfied by adopting Φ composed of instances of a collection of i.i.d. random variables, such as a set of random antipodal sequences (equal probability to present -1 or $+1$). In this situation the reconstruction is guaranteed with high probability by adopting $M \geq M_{\min} = 4K\log(N/K)$ [9].

To further compress the data, the CS theory was expanded with an innovative approach based on the concept of rakeness [14]. The considered scenario is characterized by another assumption on the acquired class of signals: the input instances are sparse and localized, i.e. the information content is non-uniformly distributed in the whole signal domain (as it almost always happens when dealing with real world signals [13]). The idea is to increase the average energy to collect ("rake") when the input signal is projected onto the sensing matrix, preserving at same time the RIP of the corresponding operator A. By exploiting this approach it is possible to reduce $M_{\min}$ guaranteeing at the same time a correct reconstruction [14].

Considering two stochastic processes $\underline{\phi}$ and $\underline{x}$, generating respectively the sensing vectors ϕ_j and the signals instances x, we define the rakeness ρ as

$$\rho(\underline{\phi}, \underline{x}) = \mathbf{E}_{\underline{\phi},\underline{x}}\left[|\langle\phi_j, x\rangle|^2\right]$$

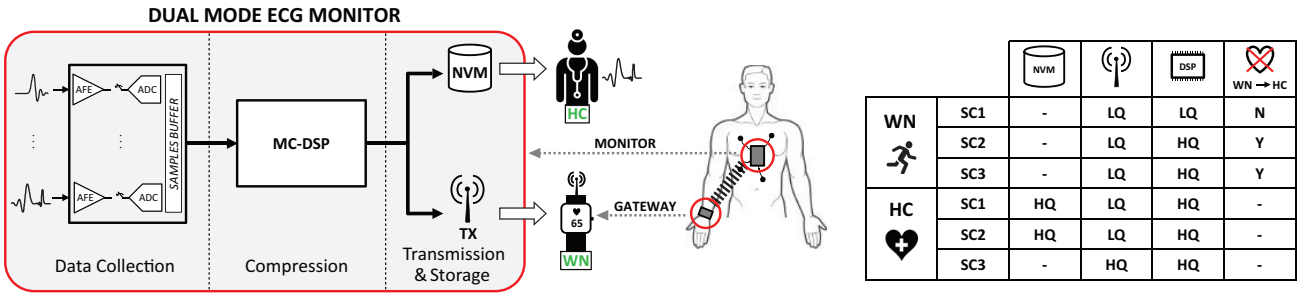

Fig. 1: WSN-based wearable biomedical system (center), dual-mode ECG monitor block scheme (left) and 3 different use case scenarios (SC1,SC2,SC3) considered for both Wellness (WN) and Healthcare (HC) applications (right).

where $\mathbf{E}_{\underline{\phi}\underline{x}}[\cdot]$ represents the expectation over the statistical characterization of stochastic processes $\underline{\phi}$ and $\underline{x}$, and $\langle\cdot,\cdot\rangle$ stands for the standard inner product such that $\langle\phi_j, x\rangle = \sum_{i=1}^{N} \phi_{j_i} x_i$. Maximizing the rakeness comes with the constraint that the sensing vectors are random enough to preserve the RIP. This is mapped into the following optimization problem:

$$\begin{aligned} \max_{\underline{\phi}} \quad & \rho(\underline{\phi}, \underline{x}) \\ \text{s.t.} \quad & \langle \phi_j, \phi_j \rangle = e \\ & \rho(\underline{\phi}, \underline{\phi}) \leq \tau e^2 \end{aligned} \tag{3}$$

where e is the energy of each sampling vector[2], and the second constraint is an upper bound related to the randomness of the process generating ϕ_j involved in the sensing. Tuning τ on a proper range is not critical since it does not appreciably alter the overall system performance [13]. The output of this optimization problem is the second-order statistical characterization of the $\underline{\phi}$ stochastic process as its correlation matrix. The sensing function generated following the solution of (3) are the directions along which projections may want to focus, though they should remain able to explore other less energetic directions that are nonetheless important components of the overall x. In Section IV practical examples will show the benefits introduced by the rakeness with respect to standard CS for the case of ECG biosignals.

Furthermore, we are exploiting the trade-off between data compression (reduce M as possible) and the goodness of the reconstruction considering two different reconstruction quality standards:

- **HQ**: ECG instances are correctly reconstructed for healthcare (medical grade) quality.
- **LQ**: the reconstruction quality targets wellness applications (i.e. heart rate detection).

Defining the *Compression Ratio* (CR) as N/M, our aim is to exploit the achievable data compression by both standard CS approach and rakeness-based CS for HQ and LQ reconstruction quality levels. For this particular application, CS introduces an important advantage. As discussed above, for a fixed class of signals, the reconstruction quality mainly depends on the cardinality of y such that *a subset of the measurements used for HQ reconstruction can be used for the LQ standard*. Numerical results are presented in Section IV following this schema: we first test the proposed approach with synthetic signals [15], where the hearth rate is swiped in a realistic range and then we validate the LQ/HQ operative points over real traces taken from [16].

[2]for antipodal sampling sequences it is always $e = N$.

III. Dual-mode ECG Monitor

A graphical representation of the WSN-based biomedical system is presented in Figure 1 (center) where is shown the monitor, worn by the patient, and the gateway, depicted as a smartwatch. The dual-mode ECG monitor (block scheme on the left of Figure 1) is composed of three components: the Analog Front-End (AFE), the multi-core DSP (MC-DSP) and the back-end for transmission (TX) or storage in a non-volatile memory (NVM).

The input 8-lead biosignal is acquired and sampled by the AFE during the *Data Collection* phase, with a sampling frequency according to the properties of the biosignal to analyze and the accuracy needed. Once a set of new samples is ready in the AFE buffer, the samples are moved to the MC-DSP memory to perform data *Compression*. During this phase, for most of the time, the whole system is idle thus we assume a deep low power state (almost zero power) for both the DSP and the TX & NVM back-end to avoid unnecessary power consumption. In the last stage of *Transmission & Storage*, within a given time window, the compressed data are either transmitted or stored in the device for future off-line medical analysis of a recorded trace. As introduced above, the choice of a multi-core signal processor is motivated by the inherent parallel nature of biomedical monitoring, where multi-channel signal analysis is often embarrassingly parallel. We consider a MC-DSP architecture similar to the architecture presented in [10], [19], deploying 8 cores each responsible of processing a data set related to a separate input lead. Each core has segregate instruction memory, while a multi-banked single-cycle data memory acts as a L1 scratchpad memory. The communication is based on a high-bandwidth interconnection network able to support single-cycle communication between cores and memory banks [10], [18].

As described in the previous section, we consider two different reconstruction quality levels, namely HQ and LQ, to enable the dual operation. We define the system as operating in Healthcare (**HC**) when the compressed signal has HQ reconstruction quality properties, while the Wellness (**WN**) application targets the LQ reconstruction quality. To take into

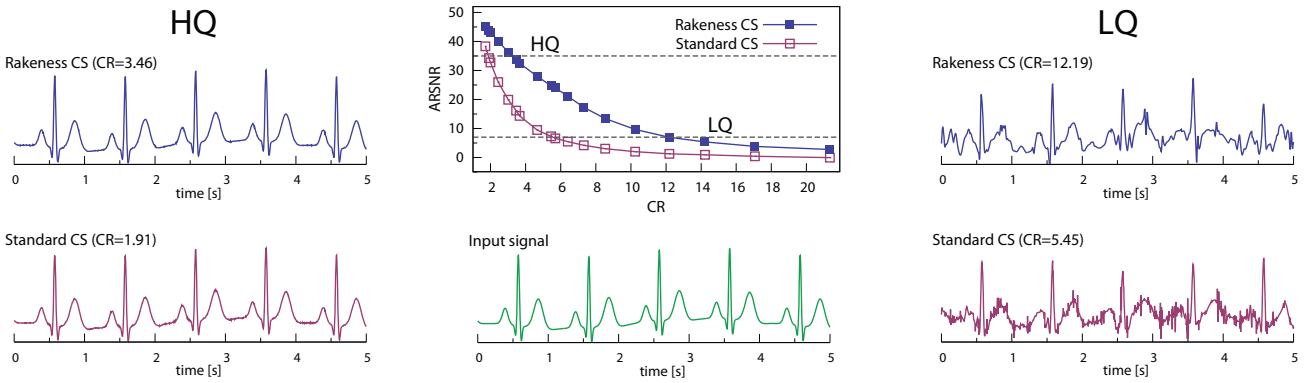

Fig. 2: ARSNR as a function of the CR (top-middle) and visual representations of the synthetic [15] input signal (bottom-middle) and reconstruction qualities for standard CS and rakeness-based CS in LQ (right) and HQ (left) operating points.

consideration different realistic applications of the proposed device, we introduce here 3 use case scenarios that differ in the quality offered and the medical usage of the device:

- **SC1** $\begin{cases} \text{WN} = \text{CS}_{\text{LQ}} + \text{TX}_{\text{LQ}} \\ \text{HC} = \text{CS}_{\text{HQ}} + \text{TX}_{\text{LQ}} + \text{NVM}_{\text{HQ}} \end{cases}$
- **SC2** $\begin{cases} \text{WN} = \text{CS}_{\text{HQ}} + \text{TX}_{\text{LQ}} + \text{BUF}_{\text{HQ}}^{\text{1min}} \\ \text{HC} = \text{CS}_{\text{HQ}} + \text{TX}_{\text{LQ}} + \text{NVM}_{\text{HQ}} \end{cases}$
- **SC3** $\begin{cases} \text{WN} = \text{CS}_{\text{HQ}} + \text{TX}_{\text{LQ}} + \text{BUF}_{\text{HQ}}^{\text{1min}} \\ \text{HC} = \text{CS}_{\text{HQ}} + \text{TX}_{\text{HQ}} \end{cases}$

where $\text{BUF}_{\text{HQ}}^{\text{1min}}$ refers to a circular buffer, located inside the MC-DSP memory, capable of storing the last observed minute in high-quality to record the transition event from WN to HC operation. We have to stress the fact that the external input can be activated by the patient with arrhythmia symptoms, therefore it is extremely important to track the event, nevertheless we consider it an optional feature (SC2 and SC3). The scheme in Figure 1 (right) summarizes the behavior of the system in the three considered scenarios, where the notation WN→HC implies the buffer to record the triggering event.

IV. Evaluation

In this section we first present the performance of the different CS approaches in terms of CR for both HQ and LQ operative points. Then we introduce the simulation framework and the evaluation in terms of energy efficiency is presented.

A. Reconstruction Quality

As mentioned above the first step of this analysis is to individuate the maximum CR associated to both CS approach for HQ and LQ operative points. This is done by adopting as input signals synthetic ECGs generated by [15] with the same settings described in [14] where, as represented in (1), an additive white Gaussian noise is added to take into account the quantization error and other non-idealities. The additive noise is such that the Intrinsic Signal to Noise Ratio (ISNR) is equal to $45\,\text{dB}$. The considered setup is characterized by time windows of $1\,\text{second}$ and input signals are sampled at $256\,\text{Hz}$ leading to $N = 256$. Moreover, in our simulation settings the heart rate of each instance is randomly fixed in the range $40\,\text{Hz} \div 120\,\text{Hz}$. The used sparsity basis is the orthonormal Symmlet-6 and all sensing functions ϕ_j are composed by antipodal values. All results are obtained by performing Monte Carlo simulations over 600 trials, where input signal reconstruction is obtained by solving (2) adopting the SPGL1 optimization toolbox[3]. As a first figure of merit we consider the Average Reconstruction Signal to Noise Ratio (RSNR) expressed by

$$\text{ARSNR} = \mathbf{E}_{\Phi,x}\left[\left(\frac{\|x\|_{l_2}}{\|x-\hat{x}\|_{l_2}}\right)_{\text{dB}}\right]$$

For the standard CS approach we always adopt an i.i.d. antipodal random sensing matrix Φ [11], while for the rakeness-based CS we first solve the optimization problem (3), whose solution is the correlation matrix to be imposed at the antipodal random ϕ_j characterizing the rakeness-based CS. Furthermore, Linear probability Feedback Process [17] is considered for the generation of the sensing matrix Φ with the prescribed correlation matrix (see [14] for more details).

The resulting ARSNR as a function of CR is shown in the top-middle plot of Figure 2. Starting from an ISNR $= 45\,\text{dB}$ we mark as HQ all cases characterized by ARSNR $\geq 35\,\text{dB}$, considering $10\,\text{dB}$ loss as the price paid for data compression. The associated minimum CRs are 1.91 for standard CS and 3.46 for rakeness-based CS. A visual representation of 5 seconds of reconstructed signal for both CS approaches is also shown in Figure 2. It is important to remark here that an increase of CR directly translates into a reduction of the amounts of bits to be transmitted or stored. Moreover, the reduced M implies a reduction of the computational load and the memory footprint required by each processing element to compute its own measurement vector y. This result highlights the improvement introduced by the rakeness-based CS in terms of CR for a fixed quality level. In Figure 2 we also observe an appreciable increase of the CR associated to rakeness-based CS on the whole range with respect to standard CS, especially for low ARSNR values.

This last consideration motivates the idea behind the second proposed classification. As mentioned before we characterize

[3] http://www.cs.ubc.ca/~mpf/spgl1.

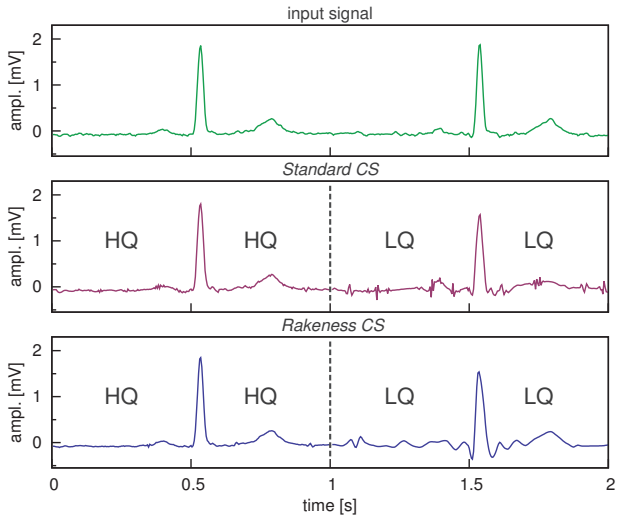

Fig. 3: Visual representation of the reconstruction quality (ECG from [16]) for both CS approaches operating in LQ and HQ.

our architecture with a LQ operative point when the reconstruction quality is fixed by a correct heart rate estimation, i.e., the amount of extracted signal information is enough for the ECG peaks detection. To determine the minimum amount of measurement needed we adopted an automatic tool for RR peaks interval detection named ecgBag[4]. In our exploration, for a fixed CR value and for both CS approaches, we ran the ecgBag tool over 600 seconds of reconstructed signal and mark the detection as good if the detection rate is over 98% of the detected peaks. This rate is always reached with ARSNR $\geq 7\,\mathrm{dB}$ that correspond to CR $= 5.45$ for standard CS and CR $= 12.19$ for rakeness-based CS. This last result shows that the rakeness-based CS is able to capture a greater part of signal information content even with very high CR values. This is confirmed by the reconstructed signals in LQ operative point, for both CS approaches, reported in Figure 2 (right). As a final remark, Table I summarize the obtained system parameters. To consolidate the analysis, the proposed settings were tested with real ECGs taken from Physionet [16], confirming the goodness of the proposed approach (see Figure 3).

TABLE I: CR for both CS approaches targeting HQ and LQ.

CS	HQ	LQ
Standard	CR $= 1.91$	CR $= 5.45$
Rakeness	CR $= 3.46$	CR $= 12.19$

B. Energy Consumption

To translate the benefits introduced by the rakeness-based CS to system-wise energy efficiency, we analyzed the energy required to compress and transmit or store a one second window data, according to the different use case scenarios and LQ/HQ operative points as introduced in the previous section.

The multi-core DSP architecture has been modeled and integrated in a SystemC-based cycle-accurate virtual platform [21], with back-annotated power numbers for the architectural elements extracted from a RTL-equivalent architecture [20]. For the power numbers we are considering the design corner (RVT,25 C,0.6 V) @ 10 MHz in a 28 nm FDSOI technology. To reduce the leakage contribution during the idle phases, we consider a reverse body bias voltage $V_{RBB} = 1\,\mathrm{V}$, leading to 7x leakage power reduction [22]. Moreover, considering that the compression task is memory-bound by nature, the requirements in terms of core-memory bandwidth imply higher supply voltage for the memory ($0.8\,\mathrm{V}$) in order to sustain the throughput. The execution time discrepancy between the SystemC and the RTL platforms is less than 7%. The multi-core DSP is operating in a SIMD fashion where each core is compressing the input data related to the associated input channel. Details on the algorithmic implementation of the CS versions can be found in [10].

[4]http://www.robots.ox.ac.uk/~gari/CODE/ECGtools/.

TABLE II: Execution cycles and memory footprint requirements for both CS approaches in LQ/HQ operative points.

	CS	Time (cycles)	Output	Sensing
LQ	Standard	109642	752B	11.75KB
	Rakeness	49048	336B	5.25KB
HQ	Standard	312246	2144B	33.5KB
	Rakeness	172428	1184B	18.5KB

We consider a 1 KB instruction memory and a stack portion of $512\,\mathrm{B}$ per core. The data memory has to allocate the input samples, considering $256\,\mathrm{samples/s}$, 8 channels and 12-bit ADC resolution, this setup leads to 4KB. Static data allocation is performed by means of cross-compiler attributes and linker script sections. The remaining memory footprint contributions (output and sensing data structures) are shown in Table II, along with the execution cycles required to perform CS considering both approaches and the HQ/LQ operative points. As already highlighted in the previous section, the sensing matrix for LQ quality standard consists of a subset of the HQ sensing matrix, therefore limiting the overhead of the dual-mode operation. Considering scenarios SC2 and SC3, the impact of the buffer to track the transition event ($\mathrm{BUF}_{\mathrm{HQ}}^{1\mathrm{min}}$) corresponds to $69.4\,\mathrm{KB}$, such extra requirement can be partially compensated by the further compression levels achieved by the rakeness-based CS w.r.t. standard CS. Moreover, as can be seen from the execution time figures (Table II), the benefits of the rakeness-based approach are two-fold: the higher compression ratio reduces the memory requirements, on the other hand the reduced execution (up to $\approx 55\%$ reduction for LQ quality) positively affects the computation costs.

To complete the analysis, we evaluated the energy requirements of the last stage of the considered biomedical monitor. For the transmission sub-system we consider a Bluetooth Low Energy (LE) transceiver for body-area networks. The figure of merit to compute the energy requirements, according to the number of bits to transmit, is $E_{TX} = 5\,\mathrm{nJ/bit}$ [23] while for the storage technology we consider a storage cost per bit $E_{NVM} = 0.1\,\mathrm{nJ/bit}$ [24]. The AFE contribution is not affected by the compression ratio and we suppose it does not represent a dominating offset, therefore is not taken into account in this analysis. The results of the evaluation are shown in Figure 4 where is presented the energy consumed in the different use

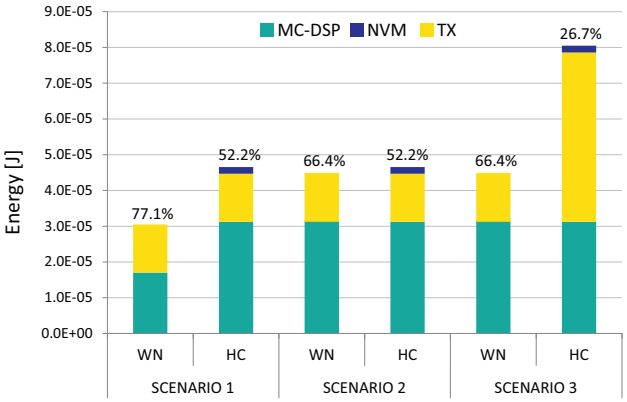

Fig. 4: Energy/1 sec-window for the different scenarios (SC1,SC2,SC3) and operation modes (HC,WN).

case scenarios (SC1,SC2,SC3) operating in the HC and WN modalities during a 1 sec compression window. The plotted bars report the stacked contribution of the MC-DSP and the NVM & TX back-end. On top of each bar are shown the energy gains taking as the baseline a biomedical system performing standard CS and transmitting in HQ the compressed ECG data.

Finally, to relate these results to a realistic usage of the dual-mode ECG monitor, we consider 75% of the time spent in WN mode, while 25% of the time is spent in HC mode. The energy efficiency improvements, with respect to the baseline, are reported in Table III.

TABLE III: Energy gains considering a realistic case (75% of the time in WN) for the 3 scenarios (SC1,SC2,SC3).

	SC1	SC2	SC3
Energy gain	70.86%	62.81%	56.49%

V. Conclusions

The recently proposed Rakeness-based CS expands the standard CS paradigm deploying the localization of input signal energy to further increase data compression without sensible RSNR degradation. We specialize the sensing stage to achieve signal qualities suitable for both Healthcare and Wellness applications, according to an external input (e.g. the patient). In this paper we envision a dual-operation wearable ECG monitor, considering a multi-core DSP for input biosignal compression and different technologies for either transmission or local storage. The experimental results show the effectiveness of the Rakeness approach (up to $\approx 70\%$ more energy efficient than the baseline) and evaluate the energy gains considering different use case scenarios.

Acknowledgment

This work was supported by the FP7 project PHIDIAS (g.a. 318013) and the ICYSoC RTD project (no. 20NA21 150939), evaluated by the Swiss NSF and funded by Nano-Tera.ch with Swiss Confederation financing.

References

[1] WHO [Online] http://www.who.int/mediacentre/factsheets/fs317.

[2] Shoaib M. et al., *"A 0.6107 W Energy-Scalable Processor for Directly Analyzing Compressively-Sensed EEG"*, In: Circuits and Systems I: Regular Papers, IEEE Transactions on , vol.61, no.4, pp.1105,1118, April 2014.

[3] Chen F. et al., "*Design and Analysis of a Hardware-Efficient Compressed Sensing Architecture for Data Compression in Wireless Sensors*", In: Solid-State Circuits, IEEE Journal of , vol.47, no.3, pp.744,756, March 2012.

[4] SmartCardia Inc. [Online] http://smartcardia.com

[5] Apple Inc. [Online] http://www.apple.com/watch

[6] Kay Misha, "*mHealth: New horizons for health through mobile technologies*",. In: World Health Organization (2011).

[7] Brignole M. et al., "*Indications for the use of diagnostic implantable and external ECG loop recorders*", In: Europace 11.5 (2009): 671-687.

[8] Mamaghanian H. et al., *"Compressed sensing for real-time energy-efficient ECG compression on wireless body sensor nodes"*, In: IEEE Transactions Biomedical Engineering, vol. 58, no.9 pp. 2456–2466, 2011.

[9] Donoho D. L., *"Compressed Sensing"*, In: IEEE Transactions on Information Theory, vol. 52, no. 4, pp. 1289–1306, Apr. 2006.

[10] Bortolotti D. et al., *"Rakeness-based Compressed Sensing on Ultra-Low Power Multi-Core Biomedical Processors"*, In: Proceedings of DASIP, 2014.

[11] Haboba J. et al., *"A pragmatic Look at Some Compressive Sensing Architectures with Saturation and Quantization"*, In: IEEE Journal on Emerging and Selected Topics in Circuits and Systems, vol. 2, n. 3, pp. 443-459, 2012.

[12] Candes E. J., *"The restricted isometry property and its implications for compressed sensing"*, In: Comptes Rendus Mathematique, vol. 346, no. 9, pp. 589–592, 2008.

[13] Cambareri V. et al., *"A rakeness-based design flow for Analog-to-Information conversion by Compressive Sensing"*, Circuits and Systems (ISCAS), 2013 IEEE International Symposium on , pp.1360–1363, May 2013.

[14] Mangia M. et al., *Rakeness in the design of analog-to-information conversion of sparse and localized signals*, In: IEEE Transactions on Circuits and Systems I: Regular Papers, vol. 59, no. 5, pp. 1001–1014, May 2012.

[15] McSharry P. E. et al., *"A dynamical model for generating synthetic electrocardiogram signals"*, In: Biomedical Engineering, IEEE Transactions on 50.3 (2003): 289-294.

[16] Goldberger A. L. et al., *"PhysioBank, PhysioToolkit, and PhysioNet: Components of a new research resource for complex physiologic signals"*, In: Circulation, vol. 101, no. 23, pp. e215e220, 2000.

[17] Rovatti R. et al., *"Memory-antipodal processes: Spectral analysis and synthesis"*, In: Circuits and Systems I: Regular Papers, IEEE Transactions on, vol. 56, no. 1, pp. 156–167, Jan. 2009.

[18] Bortolotti D. et al., *"Hybrid memory architecture for voltage scaling in ultra-low power multi-core biomedical processors"*, In: Proceedings of the ACM/IEEE DATE, 2014.

[19] Bortolotti D. et al., *"Approximate compressed sensing: ultra-low power biosignal processing via aggressive voltage scaling on a hybrid memory multi-core processor"*, In: Proceedings of ISLPED, 2014.

[20] Gautschi M. et al., *"Customizing an Open Source Processor to Fit in an Ultra-Low Power Cluster with a Shared L1 Memory"*, In: Proceedings of GLSVLSI 2014.

[21] Bortolotti D. et al., *"VirtualSoC: a Full-System Simulation Environment for Massively Parallel Heterogeneous System-on-Chip"*, In: Proceedings of IPDPWS 2013.

[22] Jacquet D. et al., "*A 3 GHz Dual Core Processor ARM Cortex TM -A9 in 28 nm UTBB FD-SOI CMOS With Ultra-Wide Voltage Range and Energy Efficiency Optimization*", In: Solid-State Circuits, IEEE Journal of , vol.49, no.4, pp.812,826, April 2014.

[23] Liu Y. et al., *"A 1.9 nJ/b 2.4 GHz multistandard (Bluetooth Low Energy/Zigbee/IEEE802. 15.6) transceiver for personal/body-area networks"*, In: Proceedings of ISSCC, 2013.

[24] Shum, D. et al., *"Highly Reliable Flash Memory with Self-Aligned Split-Gate Cell Embedded into High Performance 65nm CMOS for Automotive & Smartcard Applications"*, In: Proceedings of IMW, 2012.